JOURNAL OF SOLID STATE CHEMISTRY **122,** 251–258 (1996)
ARTICLE NO. 0110

One-Dimensional Vanadium Oxide Chains Containing Covalently Bound Copper Coordination Complexes: Hydrothermal Synthesis and Characterization of $Cu(H_2N(CH_2)_2NH_2)[V_2O_6]$, $Cu(C_{10}H_8N_2)[V_2O_6]$, and $Cu(C_{10}H_8N_2)_2[V_2O_6]$

Jeffrey R. D. DeBord,*,† Yiping Zhang,* Robert C. Haushalter,*,[1] Jon Zubieta,† and Charles J. O'Connor‡

*NEC Research Institute, 4 Independence Way, Princeton, New Jersey 08540; †Department of Chemistry, Syracuse University, Syracuse, New York 13244; and ‡Department of Chemistry, University of New Orleans, New Orleans, Louisiana 70148

Received October 3, 1995; accepted November 21, 1995

The hydrothermal reactions of $CuCl_2 \cdot 2H_2O$, V_2O_5, and bidentate amines (2,2′-dipyridyl or ethylenediamine) gave the three new one-dimensional (1-D) vanadium oxide chain compounds, $Cu(H_2N(CH_2)_2NH_2)[V_2O_6]$, 1, $Cu(C_{10}H_8N_2)[V_2O_6]$, 2, and $Cu(C_{10}H_8N_2)_2[V_2O_6]$, 3, which contain copper coordination complexes covalently bound to vanadium oxide chains. All were structurally characterized via single-crystal X-ray diffraction. Crystal data are as follows: 1, monoclinic, space group $P2_1/n$ (No. 14) with $a = 5.772(2)$ Å, $b = 8.143(3)$ Å, $c = 17.483(2)$ Å, $\beta = 90.43(2)°$, $Z = 4$, $\rho_{calc} = 2.599$ g/cm^3, and $R(R_w) = 0.029$ (0.028); 2, triclinic, space group $P\bar{1}$ (No. 2) with $a = 10.114(2)$ Å, $b = 10.839(3)$ Å, $c = 5.810(3)$ Å, $\alpha = 94.75(3)°$, $\beta = 101.16(3)°$, $\gamma = 89.81(2)°$, $Z = 2$, $\rho_{calc} = 2.27$ g/cm^3, and $R(R_w) = 0.035$ (0.044); 3, monoclinic, space group $P2_1/a$ (No. 14) with $a = 10.478(2)$ Å, $b = 13.779(2)$ Å, $c = 14.513(3)$ Å, $\beta = 100.39(1)°$, $Z = 4$, and $\rho_{calc} = 1.849$ g/cm^{-3} with $R(R_w) = 0.033$ (0.034). While compounds 1 and 2 contain almost identical 1-D metal oxide chains composed of corner-sharing VO_4 tetrahedra with one oxygen atom from each tetrahedron bound to the copper complex, complex 3 consists of 1-D chains with a $Cu(C_{10}H_8N_2)_2$ fragment bonded to every other VO_4. Temperature-dependent magnetic measurements of 1 exhibit a maximum at 20 K, while 2, which possesses well-separated Cu^{2+} centers, displays Curie–Weiss behavior from 5 to 300 K. © 1996 Academic Press, Inc.

INTRODUCTION

Vanadium oxides have been widely studied, and many different structure types and bonding geometries have been observed. Among these are the many stoichiometric and nonstoichiometric vanadium oxides, such as $VO_{0.5-1.25}$ (1), V_2O_3 (2), V_3O_5 (3), V_4O_7 (4), V_6O_{13} (5), V_4O_9 (6), V_3O_7 (7), and V_2O_5 (8). Vanadium bronzes (9) are another well-known class of vanadium oxides. In addition to these solid state compounds with extended lattices, many molecular isopolyvanadates and heteropolyanions also exist (10). Along with these 3-D, 2-D, and molecular vanadium oxide structures, several materials consisting of 1-D vanadium oxide chains, such as KVO_3, $NaVO_3$, NH_4VO_3 (11), and $[VO(VO_3)_6(VO(C_{10}H_8N_2)_2)_2]$, are known (12). We report here the hydrothermal synthesis and structural characterization by single-crystal X-ray diffraction of the three new 1-D vanadium oxides, $Cu(H_2N(CH_2)_2NH_2)$ $[V_2O_6]$, **1**, $Cu(C_{10}H_8N_2)[V_2O_6]$, **2**, and $Cu(C_{10}H_8N_2)_2$ $[V_2O_6]$, **3**. These compounds share a common structural feature of a 1-D chain of corner-sharing VO_4 tetrahedra, with $Cu(H_2N(CH_2)_2NH_2)$, $Cu(C_{10}H_8N_2)$, or $Cu(C_{10}H_8N_2)_2$ fragments covalently bound to oxygen atoms of the chain for **1**, **2**, or **3**, respectively. Compounds **1** and **2** possess almost identical 1-D chains, with one oxygen from each VO_4 tetrahedra in the vanadium oxide chain involved in bonding with the copper coordination complex, while **3** forms a 1-D vanadium oxide chain with an oxygen atom from every other vanadium site in the chain forming a bond with the $Cu(C_{10}H_8N_2)_2$ moiety. The only structurally related material reported to date is $[Cu(NH_3)_2]$ $[(VO_3)_2]$, which consists of infinite chains of corner-sharing $\{VO_4\}$ tetrahedra, linked through $\{CuO_4N_2\}$ octahedra (18).

EXPERIMENTAL SECTION

Synthesis. Reagent grade chemicals were used as received. The hydrothermal reactions were carried out in polytetrafluoroethylene-lined stainless steel containers un-

[1] To whom correspondence should be addressed.

0022-4596/96 $18.00

TABLE 1
Crystallographic Data for $Cu(H_2N(CH_2)_2NH_2)[V_2O_6]$ 1, $Cu(C_{10}H_8N_2)[V_2O_6]$ 2, and $Cu(C_{10}H_8N_2)_2[V_2O_6]$ 3

	1	2	3
Empirical formula	$Cu(H_2N(CH_2)_2NH_2)[V_2O_6]$	$Cu(C_{10}H_8N_2)[V_2O_6]$	$Cu(C_{10}H_8N_2)_2[V_2O_6]$
fw (g/mol)	321.52	471.61	573.80
Color	Green	Green	Blue
Size (mm)	0.20 × 0.15 × 0.05	0.06 × 0.100 × 0.460	0.08 × 0.12 × 0.20
Reflections measured	2802	2347	4505
Reflections ($I \geq 3\sigma(I)$)	1427	1799	2366
$2\theta_{Max}$ (deg)	60	60	50
Crystal system	Monoclinic	Triclinic	Monoclinic
Space group	$P2_1/n$	$P\bar{1}$	$P2_1/a$
a (Å)	5.772(2)	10.114(2)	10.478(2)
b (Å)	8.143(3)	10.839(2)	13.779(2)
c (Å)	17.483(2)	5.810(3)	14.513(2)
α (deg)	—	94.75(3)	—
β (deg)	90.43(2)	101.16(3)	100.39(1)
γ (deg)	—	89.81(2)	—
V (Å^3)	821.6(4)	622.7(4)	2061.0(6)
T (°C)	20	20	20
Z	4	2	4
ρ_{calc} (g/cm^3)	2.599	2.227	1.849
$\mu_{MoK\alpha}$ (cm^{-1})	47.91	31.90	19.59
Δ (σ max)	0.00	0.01	0.01
$\Delta\rho$ (e Å^{-3}) (max, min)	0.60(−0.49)	0.56(−0.52)	0.32(−0.44)
$R(F_0)^a$	0.029	0.035	0.033
$R_w(F_0)^b$	0.028	0.044	0.034

[a] $R = \Sigma||F_0| - |F_c||/\Sigma|F_0|$.
[b] $R_w = \Sigma_w(||F_0| - |F_c||)^2/\Sigma|F_0|^2$.

der autogenous pressure with a fill factor of approximately 40%.

$Cu(H_2N(CH_2)_2NH_2)[V_2O_6]$, 1. The hydrothermal reaction of V_2O_5 (0.51 g), $CuCl_2 \cdot 2H_2O$ (0.18 g), ethylenediamine (0.45 mL) and H_2O (8.0 mL) in a mole ratio of 3:1:6:444 in a 23-mL vessel at 125°C for 96 h gave dark-green prismatic crystals of **1** (47% yield based on V). The X-ray powder diffraction pattern of the bulk material showed it to be identical with the simulated pattern generated from coordinates obtained from the single-crystal X-ray data.

$Cu(C_{10}H_8N_2)[V_2O_6]$, 2. The hydrothermal reaction of V_2O_5 (0.097 g), CuO (0.045 g), 2,2′-dipyridyl (0.061 g), and H_2O (10.0 mL) in a mole ratio of 1.0:1.1:0.7:1041 in a 23-mL vessel at 150°C for 90 h gave green rod-shaped crystals of **2** (43% yield based on V) as the major product with a small amount (~5%) of an uncharacterized yellow powder.

$Cu(C_{10}H_8N_2)_2[V_2O_6]$, 3. The hydrothermal reaction of V_2O_5 (0.099 g), CuO (0.086 g), 2,2′-dipyridyl (0.316 g), and H_2O (10.0 mL) in a mole ratio of 1.0:1.8:3.7:1020 in a 23-mL vessel at 140°C for 20 h followed by heating at 150°C for 23 h gave blue prismatic crystals of **3** (54% yield based on V) as the major product along with a small amount (~5%) of an uncharacterized light blue powder.

Crystallography. The crystallographic data for all three compounds were collected on a Rigaku AFC7R four-circle diffractometer at 20°C with graphite monochromated Mo$K\alpha$ radiation and a RU300 18kW rotating anode using ω–2θ scans. In all cases, the intensities of three check reflections were monitored every 150 reflections and no decay corrections were applied. An empirical absorption correction based on azimuthal scans of several reflections was applied in the structure determinations of **1** and **3**. For **1**, the transmission factors ranged between 0.89 and 1.00, while they ranged between 0.93 and 1.00 for **3**. An empirical absorption correction using the program DIFABS (13) was applied to **2**, which resulted in transmission factors ranging from 0.39 to 1.38. The data for all structures were corrected for Lorentz and polarization effects. All three structures were solved by direct methods and all nonhydrogen atoms refined anisotropically using the teXsan crystallographic software package from the Molecular Structure Corp., The Woodlands, TX. Neutral atom scattering factors were taken from Cromer and Waber (14) and values of $\Delta f'$ and $\Delta f''$ are from Creagh and McAuley (15). The structures were minimized on Σw $(|F_o| - |F_c|)^2$, where $w = 1/\sigma^2(F_o) = 4(F_o)^2/\sigma^2(F_o^2)$. The complete data collection

TABLE 2
Positional Parameters and *B*(eq) for $Cu(H_2N(CH_2)_2NH_2)[V_2O_6]$ 1, $Cu(C_8H_{10}N_2)[V_2O_6]$ 2, and $[Cu(C_8H_{10}N_2)_2V_2O_6]$ 3

Atom	*x*	*y*	*z*	*B*(eq)
		Compound **1**		
Cu(1)	0.05908(9)	0.17095(7)	0.54488(3)	1.25(2)
V(1)	−0.2825(1)	0.3951(1)	0.43533(4)	1.03(3)
V(2)	0.1955(1)	0.2426(1)	0.37056(4)	1.14(3)
O(1)	−0.0403(5)	0.3854(4)	0.3724(2)	1.5(1)
O(2)	−0.2879(6)	0.5804(4)	0.4686(2)	2.0(1)
O(3)	0.1878(5)	0.1449(4)	0.2905(2)	2.1(1)
O(4)	0.1495(5)	0.1038(4)	0.4404(2)	1.4(1)
O(5)	−0.2343(5)	0.2576(4)	0.5046(2)	1.5(1)
O(6)	0.4713(5)	0.3417(4)	0.3785(2)	1.9(1)
N(1)	0.3528(6)	0.0812(5)	0.5876(2)	1.6(2)
N(2)	−0.0167(6)	0.2304(5)	0.6519(2)	1.9(2)
C(1)	0.3357(8)	0.0745(7)	0.6715(3)	2.3(2)
C(2)	0.1993(9)	0.2181(6)	0.6984(3)	2.2(2)
		Compound **2**		
Cu(1)	0.26175(7)	0.07956(6)	0.5282(1)	1.51(3)
V(1)	0.2277(1)	−0.20496(9)	0.3148(2)	1.34(3)
V(2)	0.0959(1)	−0.11930(9)	0.7665(2)	1.37(3)
O(1)	0.3216(4)	−0.0771(4)	0.3981(7)	1.8(1)
O(2)	0.1272(4)	−0.1992(4)	0.0268(7)	2.0(2)
O(3)	0.3280(5)	−0.3212(4)	0.3056(8)	2.4(2)
O(4)	0.1245(4)	−0.2249(4)	0.5273(7)	1.9(2)
O(5)	0.2022(4)	−0.0007(4)	0.7789(7)	2.0(2)
O(6)	0.0606(4)	0.0743(5)	0.2862(8)	2.8(2)
N(1)	0.3649(5)	0.1779(4)	0.3473(9)	1.7(2)
N(2)	0.2247(5)	0.2474(4)	0.6608(9)	1.5(2)
C(1)	0.3531(6)	0.3008(5)	0.384(1)	1.6(2)
C(2)	0.4162(6)	0.3815(6)	0.264(1)	2.1(2)
C(3)	0.4933(7)	0.3332(6)	0.109(1)	2.4(2)
C(4)	0.5042(7)	0.2073(6)	0.072(1)	2.4(2)
C(5)	0.4393(6)	0.1315(6)	0.196(1)	2.2(2)
C(6)	0.2700(6)	0.3411(5)	0.557(1)	1.8(2)
C(7)	0.2400(7)	0.4625(6)	0.615(1)	2.4(2)
C(8)	0.1643(7)	0.4884(6)	0.788(1)	2.8(3)
C(9)	0.1193(7)	0.3923(6)	0.894(1)	2.5(3)
C(10)	0.1493(6)	0.2724(6)	0.823(1)	2.0(2)

TABLE 2—*Continued*

Atom	*x*	*y*	*z*	*B*(eq)
		Compound **3**		
Cu(1)	0.64695(6)	0.04796(5)	0.75418(4)	2.15(1)
V(1)	0.77238(7)	−0.16974(6)	0.74894(5)	1.85(2)
V(2)	0.57755(8)	−0.35401(6)	0.71012(6)	2.01(2)
O(1)	0.7352(3)	−0.0585(2)	0.7051(2)	2.42(8)
O(2)	0.7362(3)	−0.1764(3)	0.8523(2)	3.12(8)
O(3)	0.9404(3)	−0.1945(3)	0.7577(2)	3.15(9)
O(4)	0.6744(3)	−0.2541(2)	0.6747(2)	2.46(8)
O(5)	0.5248(4)	−0.4191(3)	0.6188(2)	3.44(9)
O(6)	0.6675(3)	−0.4226(3)	0.7873(2)	3.34(9)
N(1)	0.8063(4)	0.0809(3)	0.8429(3)	2.21(9)
N(2)	0.5677(4)	0.0819(3)	0.8722(3)	2.26(9)
N(3)	0.6196(4)	0.1854(3)	0.6857(3)	2.33(9)
N(4)	0.4879(4)	0.0218(3)	0.6600(3)	2.11(9)
C(1)	0.9246(5)	0.0738(4)	0.8224(4)	2.8(1)
C(2)	1.0348(5)	0.0946(4)	0.8872(4)	3.1(1)
C(3)	1.0215(5)	0.1219(4)	0.9771(4)	3.1(1)
C(4)	0.8982(5)	0.1288(4)	0.9980(3)	2.7(1)
C(5)	0.7922(5)	0.1081(3)	0.9307(3)	2.0(1)
C(6)	0.6563(5)	0.1115(3)	0.9451(3)	2.1(1)
C(7)	0.6234(5)	0.1417(4)	1.0284(3)	2.8(1)
C(8)	0.4941(5)	0.1418(4)	1.0358(4)	3.4(1)
C(9)	0.4028(5)	0.1109(4)	0.9623(4)	3.2(1)
C(10)	0.4425(5)	0.0825(4)	0.8808(4)	3.0(1)
C(11)	0.6826(5)	0.2690(4)	0.7101(4)	3.1(1)
C(12)	0.6478(6)	0.3560(4)	0.6643(4)	3.3(1)
C(13)	0.5497(6)	0.3548(4)	0.5882(4)	3.4(1)
C(14)	0.4856(5)	0.2685(4)	0.5615(4)	3.1(1)
C(15)	0.5205(5)	0.1860(4)	0.6133(3)	2.1(1)
C(16)	0.4519(4)	0.0913(4)	0.5954(3)	2.0(1)
C(17)	0.3560(5)	0.0744(4)	0.5179(3)	2.7(1)
C(18)	0.2951(5)	−0.0142(4)	0.5083(4)	3.0(1)
C(19)	0.3322(5)	−0.0847(4)	0.5749(4)	3.0(1)
C(20)	0.4278(5)	−0.0642(4)	0.6495(3)	2.6(1)

Note. B_{eq} $8/3\pi^2(U_{11}(aa^*)^2 + U_{22}(bb^*)^2 + U_{33}(cc^*)^2 + 2U_{12}aa^*bb^* \cos\gamma + 2U_{13}aa^*cc^* \cos\beta + 2U_{23}bb^*cc^* \cos\alpha)$.

parameters and details of the structure solutions and refinements are summarized in Table 1. Final positional parameters of all nonhydrogen atoms are given in Table 2 and selected bond distances and bond angles are given in Table 3. For all structures, the hydrogen atoms were located from difference Fourier maps and included in the refinement with fixed positional and thermal parameters. Further crystallographic details are available as supplementary material.

Magnetic susceptibility. The magnetic susceptibility data were recorded from 2 to 300 K for **1** and from 5 to 300 K for **2** using a Quantum Design MPMS-5S SQUID susceptometer. Measurement and calibration techniques have been reported elsewhere (16). The temperature-dependent magnetic data were measured at a magnetic field of 1000 G.

RESULTS AND DISCUSSION

As with all hydrothermal syntheses, reaction products can be very sensitive to the initial reaction conditions. For the syntheses of **1**, **2**, and **3**, small changes in temperature, mole ratios, and reaction time can have great a effect on the yield and phase purity of the products. In the synthesis of **1**, both solid reactants were placed in the reaction vessel, followed by addition of water and ethylenediamine. The mixture was stirred, then heated at 125°C for 96 h. Dark-green prismatic crystals of **1** were the only solid isolated from the reaction, and the X-ray powder diffraction pattern of the bulk material was identical to the simulated pattern generated from the single-crystal X-ray data. For **2** and **3**, all of the solid reactants were placed in the reaction vessel, then the water was added. The mixtures were stirred, then heated at 150°C for 90 h in the case of **2**, while **3** was

TABLE 3
Selected Bond Lengths (Å) for $Cu(H_2N(CH_2)_2NH_2)[V_2O_6]$ 1, $Cu(C_{10}H_8N_2)[V_2O_6]$ 2, and $Cu(C_{10}H_8N_2)_2[V_2O_6]$ 3

Atom	Atom	Distance	Atom	Atom	Distance
		Compound **1**			
Cu(1)	O(4)	1.978(3)	Cu(1)	O(5)	1.960(3)
Cu(1)	N(1)	1.988(4)	Cu(1)	N(2)	1.981(4)
V(1)	O(1)	1.785(3)	V(1)	O(2)	1.621(4)
V(1)	O(5)	1.670(3)	V(1)	O(6)	1.779(3)
V(2)	O(1)	1.793(3)	V(2)	O(3)	1.610(3)
V(2)	O(4)	1.687(3)	V(2)	O(6)	1.791(3)
		Compound **2**			
Cu(1)	O(1)	1.944(4)	Cu(1)	O(5)	1.947(4)
Cu(1)	O(6)	2.236(4)	Cu(1)	N(1)	1.986(5)
Cu(1)	N(2)	1.979(5)	V(1)	O(1)	1.667(4)
V(1)	O(2)	1.788(4)	V(1)	O(3)	1.620(4)
V(1)	O(4)	1.790(4)	V(2)	O(2)	1.780(4)
V(2)	O(4)	1.794(4)	V(2)	O(5)	1.667(4)
V(2)	O(6)	1.634(4)			
		Compound **3**			
Cu(1)	O(1)	1.937(3)	Cu(1)	N(1)	1.969(4)
Cu(1)	N(2)	2.087(4)	Cu(1)	N(3)	2.134(4)
Cu(1)	N(4)	1.989(4)	V(1)	O(1)	1.678(3)
V(1)	O(2)	1.615(3)	V(1)	O(3)	1.775(3)
V(1)	O(4)	1.780(3)	V(2)	O(3)	1.830(3)
V(2)	O(4)	1.837(3)	V(2)	O(5)	1.614(3)
V(2)	O(6)	1.629(4)			

heated at 140°C for 20 h then at 150°C for 23 h. Crystals of **2** and **3** were the major solid products of these reactions. A small amount (~5%) of a uncharacterized yellow powder was also present in the synthesis of **2** while a small amount (~5%) of an uncharacterized blue powder was present in the synthesis of **3**.

The basic building block of the 1-D vanadium oxide chain as well as the atom-labeling schemes for **1** and **2**, are shown in Fig. 1. Both structures are made up of 1-D chains of corner-sharing VO_4 tetrahedra, which run parallel to the *a* axis in **1** and parallel to *c* in **2**. Figure 2 shows a polyhedral representation of the 1-D chains in **1** and **2**. In both **1** and **2**, two oxygen atoms from each VO_4 tetrahedron form the vanadium–oxygen–vanadium bonds which make up the infinite chain of corner-sharing tetrahedra, while the third oxygen atom is bound only to the vanadium atom. The fourth O atom from each VO_4 tetrahedron is shared with the copper atom. These chains of vanadium oxide tetrahedra are similar to those found in $NaVO_3$, KVO_3, and NH_4VO_3 (11). The oxygen atoms bridging the vanadium tetrahedra have bond distances between 1.803 and 1.805 Å for $NaVO_3$, KVO_3, and NH_4VO_3, while the bridging vanadium oxygen bonds are between 1.779(3) and 1.793(3) Å in **1** and **2**. The terminal vanadyl oxygen atoms in $NaVO_3$, KVO_3, and NH_4VO_3 have bond distances ranging from 1.633 to 1.647 Å, while the terminal O atoms in **1** and **2** exhibit V–O distances between 1.610(3) and 1.621(4) Å. In both **1** and **2**, oxygen atoms from two adjacent VO_4 tetrahedra form bonds with the copper atom while the bidentate ligand in each is coordinated to the remaining two sites on copper to complete the square planar configuration about the copper.

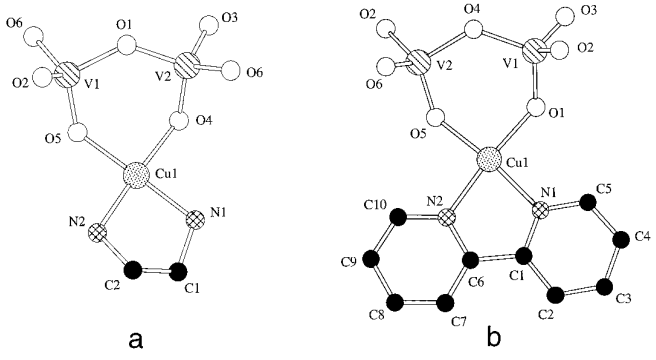

FIG. 1. Basic building block and atom labeling scheme in (a) **1** and (b) **2**, where Cu atoms are the stippled circles, V atoms are striped, O atoms are open, N atoms are cross-hatched, and C atoms are filled.

The square planar geometry about the copper atom in **1** is very close to ideal, with no deviations of more than five degrees from ideal square planar geometry. The axial distance between cooper centers on the chain is 5.482 and 3.266 Å for copper atoms in adjacent layers. While there is no bonding interaction between the copper atoms either along a chain or between chains, there are other interactions between adjacent chains which are significant. Figure 3 shows the nearest interchain copper–copper distance as well as the structurally more important interchain copper–oxygen distances. For any copper site, there are axial oxygen atoms above and below the CuO_2N_2 plane which must be considered, with oxygen atoms (O2) and (O4) from adjacent chains at 2.431(4) and 2.558(4) Å, respectively, from the copper atom. Although these contacts are not nearly as short as the equatorial Cu–O bonds, the interactions are nonetheless significant. Because of these interactions, the copper atom can also be viewed as a distorted octahedral link between the 1-D VO_4 tetrahedral chains. The bonding interactions of (O4) and Cu atoms from adjacent chains are also important because the resulting Cu–(O4)–Cu interaction could constitute the pathway for magnetic exchange that gives rise to the antiferromagnetic behavior observed in **1** discussed below. Extensive hydrogen bonding exists between the ethylenediamine fragment on one chain and the surrounding oxygen atoms. Hydrogens (H3) and (H4) on (N2) form hydrogen bonds with (O1) and (O3) of adjacent chains with nitrogen–oxygen distances of 3.174(5) and 3.142(5) Å, respectively.

As expected, the replacement of ethylenediamine with 2,2′-dipyridyl in the copper coordination complex has a

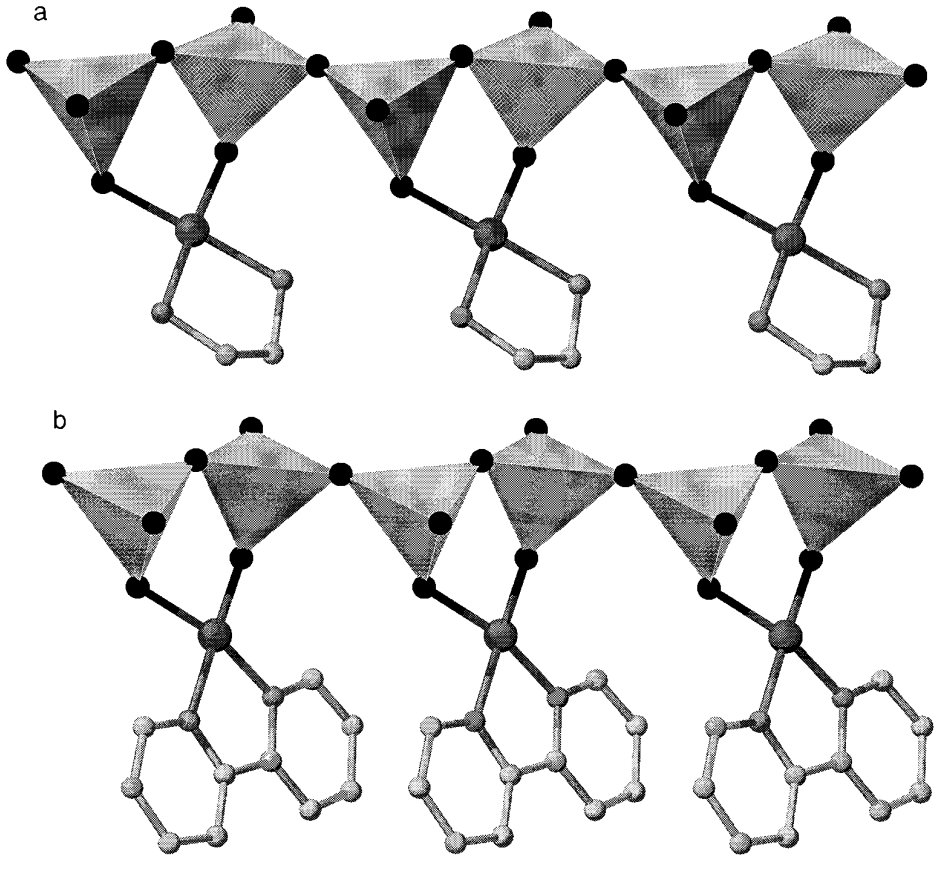

FIG. 2. View of one of the tetrahedral 1-D chains in (a) **1** and (b) **2**.

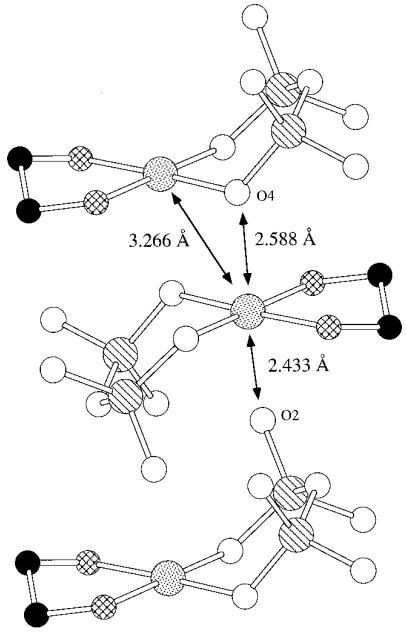

FIG. 3. Illustration of several adjacent fragments in **1** showing the closest copper–copper interaction, and the interactions of (O2) and (O4) with the copper atom of the chain in between.

profound effect on the packing of the 1-D chains in the lattice, the interchain copper–oxygen interactions, and the relative positions of the copper atoms in the crystal lattice. While the individual 1-D chains in **1** and **2** are very similar, the coordination sphere about copper in **2** is quite different from that in **1**. While **1** has two close copper–oxygen interactions axial to the square planar copper coordination complex, **2** has only one such interaction. In **2**, the axial oxygen atom from an adjacent chain is 2.236(4) Å from the copper atom, which is 0.195 Å shorter than the closest axial Cu–O contact in **1** making this Cu five coordinate. Thus, **2** can be described as pairs of 1-D chains bridged by oxygen atoms as shown in Fig. 4. The other interesting difference between **1** and **2** is the packing of the copper atoms in the crystal lattice. All copper atoms in **2** are separated from each other by at least 5.173 Å while **1** has an a much shorter copper–copper distance of 3.266 Å.

Although compound **3** is also based on 1-D chains of vanadium oxide tetrahedra, the vanadium oxide chain and the coordination sphere about copper are quite distinct from **1** and **2**. These differences are due to the volume of the two 2,2′-dipyridyl ligands bound to each copper, as the large steric requirements of the 2,2′-dipyridyl ligands cause the copper to adopt a distorted

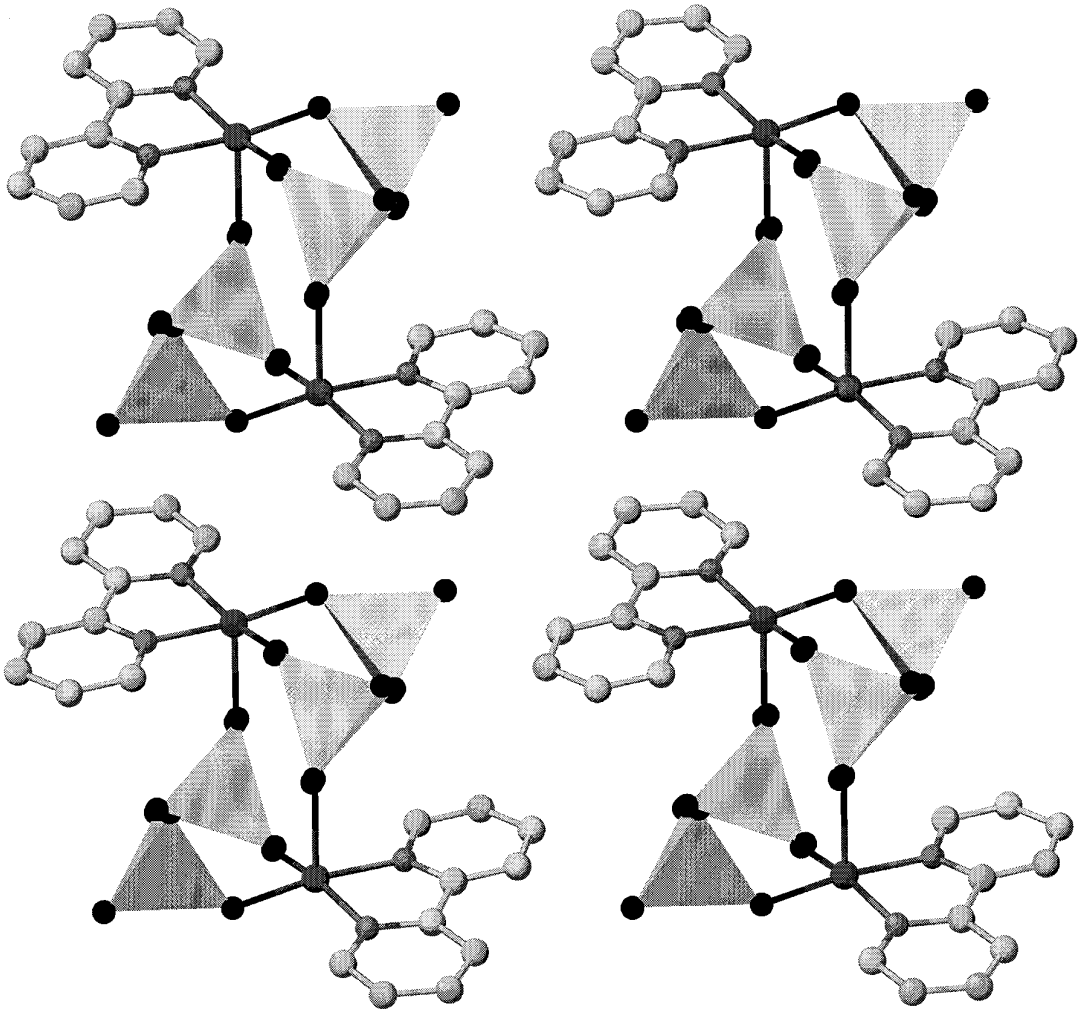

FIG. 4. A projection down the *c* axis of **2** showing the pairs of 1-D chains bridged by oxygen atoms.

trigonal biyramidal geometry similar to that seen in the structures of $[Cu(2,2'\text{-dipyridyl})_2I]^+$ and $[Cu(\text{phenanthroline})_2H_2O]^{2+}$ (17) and also permits only one oxygen from every other VO_4 tetrahedra to bind to the copper complex. This is in contrast to **1** and **2**, where oxygen atoms from adjacent tetrahedra in the vanadium oxide chain and one bidentate ligand (ethylenediamine, 2,2′-dipyridyl) adopt a square planar configuration about copper. The increased bulk of the copper coordination complex also causes the vanadium oxide chain to pack in a zigzag manner in the crystal lattice (see Fig. 5), unlike **1** and **2**, which have more linear VO_4 chains.

While the covalent attachment of transition metal complex fragments to 1-D VO_4 tetrahedral chains as seen in **1**, **2**, and **3** is unusual, it has also been observed in $[VO(VO_3)_6(VO(C_{10}H_8N_2)_2)_2]$ (11). This compound is synthesized by the hydrothermal treatment an equal molar mixture of V_2O_3 and 2,2′-dipyridyl for 48 h at 200°C. While this compound is also made up of 1-D chains, the chains are made up of two smaller chains of corner-sharing VO_4 tetrahedra with the VO_4 tetrahedral chains linked by square pyramidal vanadium sites between the chains. Every third link of the tetrahedral vanadium oxide chain contains a $VO(C_{10}H_8N_2)_2$ fragment bound to the chain through a single oxygen bridge. This is similar to **3**, where the $Cu(C_{10}H_8N_2)_2$ is bound through a single oxygen atom to every other vanadium site in the vanadium oxide chain. Both of these complexes differ from **1** and **2** in that there is one copper fragment for every other tetrahedron in the chain, and each tetrahedron of the chain has an oxygen bound to the copper-bidentate ligand fragment.

Magnetic Susceptibility

The high-temperature magnetic susceptibility data for **1** exhibits Curie–Weiss paramagnetism and was fit ($T > 25$ K) to the Curie–Weiss law. For **1**, $C = 0.426$ emu-K/mole,

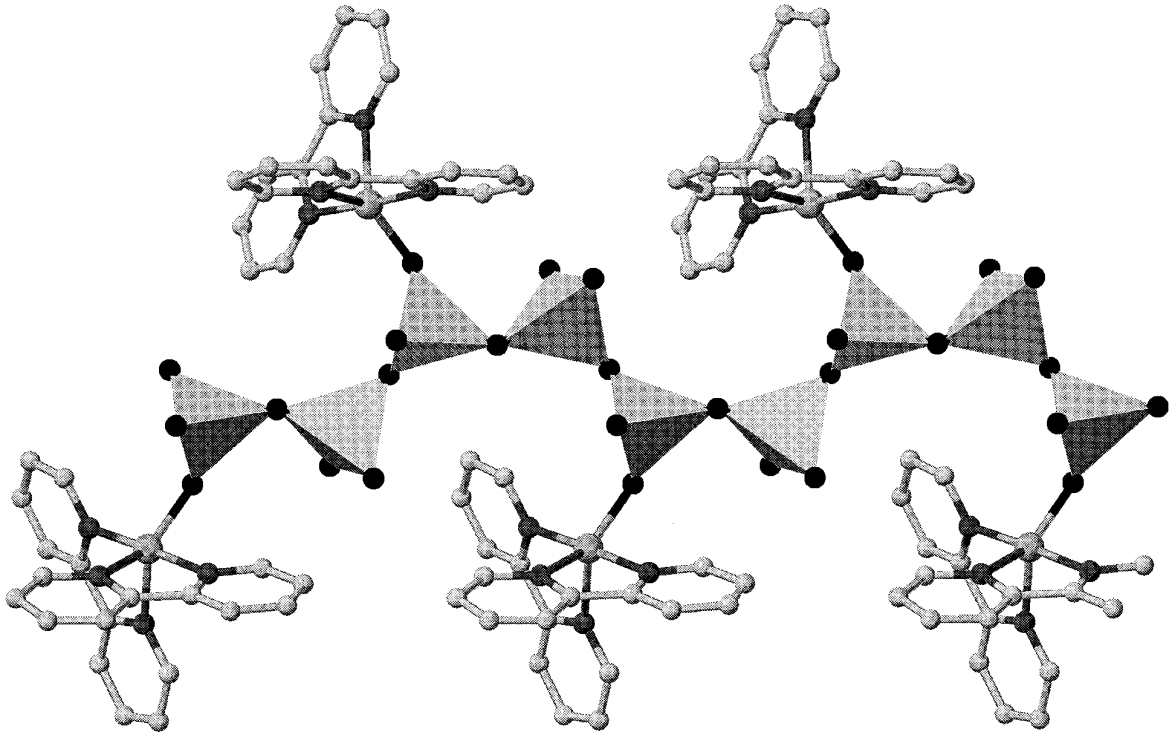

FIG. 5. View of one of the tetrahedral 1-D chains in **3**.

$\theta = -4.6$ K, and TIP = 0.00225 emu/mol. The electron structure of copper(II) and vanadium(V) corresponds to electron configurations of $3d^9$ and $3d^0$, respectively. Therefore one unpaired electron resides on the copper(II) with a g value of 2.13.

There is a maximum in the low-temperature magnetization versus temperature curve for **1** at 20 K, indicative of a moderate amount of antiferromagnetic coupling. The magnetic exchange that is expected in copper(II) with a ^{2}D free ion ground term, $3d^9$ electron structure, and spin $S = 1/2$ is the isotropic Heisenberg spin Hamiltonian given in Equation 1.

$$H = -2J\mathbf{S}_1 \cdot \mathbf{S}_2. \qquad [1]$$

Although **1** is a structural linear chain, there is a short interchain copper–copper distance of 3.266 Å while all other copper–copper distances are greater than 5.482 Å. This alternating short–long arrangement of the copper atoms allows the magnetic behavior to be modeled as a binuclear unit. The effect of the spin Hamiltonian on the behavior of a pair of interacting electrons can be expressed as follows:

$$\chi = (Ng^2\mu_\beta^2/kT)[\exp(2J/kT)/(1 + 3\exp(2J/kT)], \qquad [2]$$

where a negative J denotes a ground state singlet, the susceptibility is calculated per copper(II) atom, and all of the parameters have their usual meaning.

The magnetic susceptibility data of **1** was analyzed with this equation and the results of a least-squares fit of Eq. [2] yields the parameters $g = 2.049$, $J/k = -6.0$ K. No additional terms to correct for a temperature-independent paramagnetism were required. Although the dimers are linked in a structural linear chain, an interdimer exchange correction was not required to fit the data. The result of this fit is illustrated in Fig. 6, where magnetic susceptibility

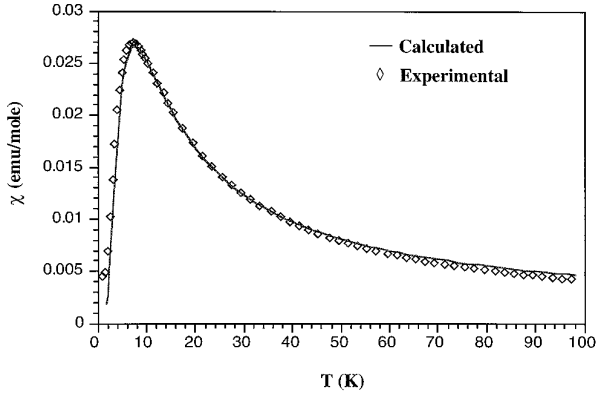

FIG. 6. Experimental (diamonds) and calculated (solid line) magnetic susceptibility for **1**.

is plotted as a function of temperature, with the smooth curve representing the theoretical calculation.

The magnetic susceptibility data for **2** exhibits Curie–Weiss paramagnetism over the entire temperature range of 5 to 300 K. The magnetic data were fit to the Curie–Weiss law with $C = 0.408$ emu-K/mole and $\theta = 0.9$ K. As in **1**, the electron structure of copper(II) and vanadium(V) correspond to electronic configurations of $3d^9$ and $3d^0$, respectively. Therefore one unpaired electron resides on the copper(II) with a g value of 2.09.

CONCLUSIONS

Several new 1-D vanadium oxides which incorporate a transition metal coordination complex covalently bound to the metal oxide chain, in this case Cu^{2+} coordinated to bidentate amines, were synthesized and structurally characterized. The complexes were synthesized hydrothermally and readily yielded single crystals from simple precursors. As with most hydrothermal syntheses, the yield and phase purity of the product are very sensitive to temperature, ratio of reactants, and reaction time. Although the number of low-dimensional vanadium oxides of this type is not yet extensive, it should be possible to substitute for copper other transition metals which adopt square planar geometry or to substitute other nitrogen donating ligands to develop a series of analogous compounds where transition metal complex fragments are covalently bonded to 1-D VO_4 tetrahedral chains. By varying the synthetic conditions of these reactions, we have also prepared a large series of compounds with transition element coordination complexes between mixed valence vanadium oxide layers. The structures and properties of these new materials will be reported shortly.

ACKNOWLEDGMENT

The work at Syracuse University was supported by NSF Grant CHE-9318824.

REFERENCES

1. (a) S. Westman and C. Nordmark, *Acta Chem. Scand.* **14,** 465 (1960); (b) G. Stenstrom and S. Westman, *Acta Chem. Scand.* **22,** 1712 (1968).
2. W. R. Robinson, *Acta Crystallogr.* **B31,** 1153 (1975).
3. S. Asbrink, *Acta Crystallogr.* **B36,** 1332 (1980).
4. H. Horiuchi, M. Tokonami, N. Morimoto, and K. Nagasawa, *Acta Crystallogr.* **B28,** 1401 (1972).
5. K. Wilhelmi, K. Waltersson, and L. Kihlborg, *Acta Chem. Scand.* **25,** 20 (1971).
6. K. Waltersson and K. Wilhelmi, *Acta Chem. Scand.* **24,** 3409 (1970).
7. K. Waltersson, B. Forslund, and K. Wilhelmi, *Acta Crystallogr.* **B30,** 2644 (1974).
8. H. G. Bachmann, F. R. Ahmed, and W. H. Barnes, *Zh. Krist.* **115,** 110 (1961).
9. (a) K. Waltersson and B. Forslund, *Acta Crystallogr.* **B33,** 775 (1977); (b) K. Waltersson and B. Forslund, *Acta Crystallogr.* **B33,** 780 (1977); (c) K. Waltersson and B. Forslund, *Acta Crystallogr.* **B33,** 784 (1977); (d) K. Waltersson and B. Forslund, *Acta Crystallogr.* **B33,** 789 (1977); (e) A. D. Wadsley, *Acta Crystallogr.* **10,** 261 (1957); (f) S. J. Hibble and P. G. Dickens, *J. Solid State Chem.* **63,** 166 (1986); (g) D. W. Murphy, P. A. Christianson, F. J. Disalvo, and J. V. Waszczak, *Inorg. Chem.* **18,** 2800 (1979); (h) D. W. Murphy and P. A. Christian, *Science* **205,** 651 (1979); (i) H. T. Evans and S. Block, *Inorg. Chem.* **5,** 1808 (1966).
10. (a) M. T. Pope, "Heteropoly and Isopoly Oxometalates." Springer Verlag, New York, 1983; (b) M. T. Pope and A. Müller, *Angew. Chem., Int. Ed. Engl.* **30,** 29 (1991); (c) A. Müller, R. Rohfling, E. Krickemeyer, and H. Bogge, *Angew. Chem., Int. Ed. Engl.* **32,** 909 (1993); (d) I. M. Kahn, Q. Chen, H. Hope, S. Parkin, C. J. O'Connor, and J. A. Zubieta, *Inorg. Chem.* **32,** 2929 (1991); (e) W. G. Klemperer, T. A. Marquart, and O. M. Yaghi, *Angew. Chem. Int. Ed. Engl.* **31,** 49 (1992).
11. (a) H. T. Evans, *Zh. Krist.* **114,** 257 (1960); (b) F. C. Hawthorne and C. Calvo, *J. Solid State Chem.* **22,** 157 (1977).
12. G. Huan, J. W. Johnson, A. J. Jacobson, and J. S. Merola, *J. Solid State Chem.* **91,** 385 (1991).
13. N. Walker and D. Stuart, *Acta Crystallogr.* **A39,** 158 (1983).
14. D. T. Cromer and J. T. Waber, "International Tables for X-ray Crystallography," Vol. IV, Table 2.2 A. Kynoch, Birmingham, England, 1974.
15. D. C. Creagh and W. J. McAuley, "International Tables for Crystallography," Vol. C, Table 4.2.6.8, p. 219. Kluwer, Boston, 1992.
16. C. J. O'Connor, *Prog. Inorg. Chem.* **29,** 203 (1982).
17. R. J. Deeth and M. Gerloch, *Inorg. Chem.* **23,** 2853 (1984).
18. S. Aschwanden, H. W. Schmalle, A. Peller, and H. R. Oswald, *Mat. Res. Bull.* **28,** 45 (1993).